PCCP

Accepted Manuscript

This article can be cited before page numbers have been issued, to do this please use: J. F. Angiolini, P. Y. Steinberg, M. Stortz, E. Mocskos, L. Bruno, G. J. D. A. A. Soler-Illia, P. C. Angelomé, A. Wolosiuk and V. Levi, *Phys. Chem. Chem. Phys.*, 2017, DOI: 10.1039/C7CP05186G.

This is an Accepted Manuscript, which has been through the Royal Society of Chemistry peer review process and has been accepted for publication.

Accepted Manuscripts are published online shortly after acceptance, before technical editing, formatting and proof reading. Using this free service, authors can make their results available to the community, in citable form, before we publish the edited article. We will replace this Accepted Manuscript with the edited and formatted Advance Article as soon as it is available.

You can find more information about Accepted Manuscripts in the author guidelines.

Please note that technical editing may introduce minor changes to the text and/or graphics, which may alter content. The journal's standard Terms & Conditions and the ethical guidelines, outlined in our author and reviewer resource centre, still apply. In no event shall the Royal Society of Chemistry be held responsible for any errors or omissions in this Accepted Manuscript or any consequences arising from the use of any information it contains.

ROYAL SOCIETY OF CHEMISTRY

rsc.li/pccp

View Article Online
DOI: 10.1039/C7CP05186G

Journal Name

COMMUNICATION

Diffusion of single dye molecules in hydrated TiO_2 mesoporous films

Received 00th January 20xx,
Accepted 00th January 20xx

DOI: 10.1039/x0xx00000x

www.rsc.org/

Juan F. Angiolini[a], Martín Stortz[b], Paula Y. Steinberg[c], Esteban Mocskos[d], Luciana Bruno[e], Galo Soler-Illia[f], Paula C. Angelomé[c], Alejandro Wolosiuk[c,g]*, and Valeria Levi [a,]*

Mesoporous oxide films are attractive frameworks in technological areas such as catalysis, sensors, environmental protection, and photovoltaics. Herein, we used fluorescence correlation spectroscopy to explore how the pore dimensions of hydrated TiO_2 mesoporous calcined films modulate the molecular diffusion. Rhodamine B molecules in mesoporous films follow a Fickian process 2-3 orders slower compared to the probe in water. The mobility increases with the pore and neck radii reaching an approximately constant value for neck radius > 2.8 nm. However, the pore size does not control the dye diffusion at low ionic strength emphasizing the relevance of the probe interactions with the pore walls on the dye mobility. In conclusion, our results show that the thermal conditioning of TiO_2 mesoporous films provides an exceptional tool for controlling the pore and neck radii in the nanometer scale and has a major impact on molecular diffusion within the mesoporous network.

Mesoporous oxide thin films (MOTF) are essential components in the materials science "toolbox" for many advanced applications including (bio)sensors, catalysts, adsorbents and controlled release devices.[1] Their high surface area / volume relation is ideal for anchoring a high density of chemical groups aimed for immobilization or controlled release of molecules and ions. On the other hand, MOTF can be easily deposited on various substrates with arbitrary shape ensuring an easy manipulation and operation in diverse reaction media. The uniform nanosized cavities allow both connectivity and diffusion of analytes along the supramolecular structure which can be chemically tailored as permselective membranes.[2] The combination of these structures with several building blocks in a hierarchical fashion leads to an integrated chemical platform that includes nanoparticles, enzymes or inorganic complexes[3-5]. Understanding the molecular transport along tortuous or highly ordered media with different pore hierarchies is extremely relevant in the context of catalysis, sensing, and separation processes as analytes must diffuse and react within the mesoporous framework. [6, 7,8, 9,10] TiO_2-based MOTF receive considerable attention as they are promising materials for photovoltaics applications, (dye-sensitized solar cells, DSSC) and photocatalytic environmental remediation.[11-13] In these applications the TiO_2-MOTF fulfill a dual purpose: i) the high surface area exposed enhance the electron exchange due to photochemical processes and ii) the mesoporous structure allows the diffusion and shuttling of redox mediators in order to complete the electron transport.[14]

Previous works have shown that the controlled Evaporation Induced Self-Assembly (EISA) synthesis of TiO_2-based MOTF has three important variables that drastically affect the pore size and connectivity: the chemical structure of the template, the aging conditions and the thermal treatment. [10, 15] These conditioning variables impact on the pore radius and the neck between the pores radius and allow the design of mesoporous TiO_2 structures with precise geometrical parameters.

[a] *Universidad de Buenos Aires, Facultad de Ciencias Exactas y Naturales, Departamento de Química Biológica, Argentina- CONICET - Universidad de Buenos Aires. Instituto de Química Biológica de la Facultad de Ciencias Exactas y Naturales (IQUIBICEN), Buenos Aires. Argentina. E-mail:vlevi12@gmail.com*
[b] *CONICET - Universidad de Buenos Aires. Instituto de Fisiología, Biología Molecular y Neurociencias (IFIBYNE), Buenos Aires, Argentina.*
[c] *Gerencia Química - Centro Atómico Constituyentes – Comisión Nacional de Energía Atómica. CONICET. Av. Gral. Paz 1499, 1650, San Martín, Pcia. Buenos Aires, Argentina. E-mail:wolosiuk@cnea.gov.ar*
[d] *Universidad de Buenos Aires. Facultad de Ciencias Exactas y Naturales. Departamento de Computación. Buenos Aires, Argentina-CONICET. Centro de Simulación Computacional para Aplicaciones Tecnológicas (CSC). Buenos Aires, Argentina*
[e] *CONICET - Universidad de Buenos Aires. Instituto de Física de Buenos Aires (IFIBA), Buenos Aires. Argentina*
[f] *Instituto de Nanosistemas, UNSAM, 25 de Mayo y Francia (1650), San Martín, Argentina*
[g] *Departamento de Química Inorgánica, Analítica y Química Física, Facultad de Ciencias Exactas y Naturales, Universidad de Buenos Aires. Ciudad Universitaria, Pab. II. C1428EHA, Buenos Aires, Argentina.*

Electronic Supplementary Information (ESI) available: experimental details for MOTF synthesis and characterization techniques: transmission electron microscopy, 2D-small angle X-ray scattering, FTIR, environmental ellipsometric porosimetry and X-ray diffraction. See DOI: 10.1039/x0xx00000x

View Article Online
DOI: 10.1039/C7CP05186G

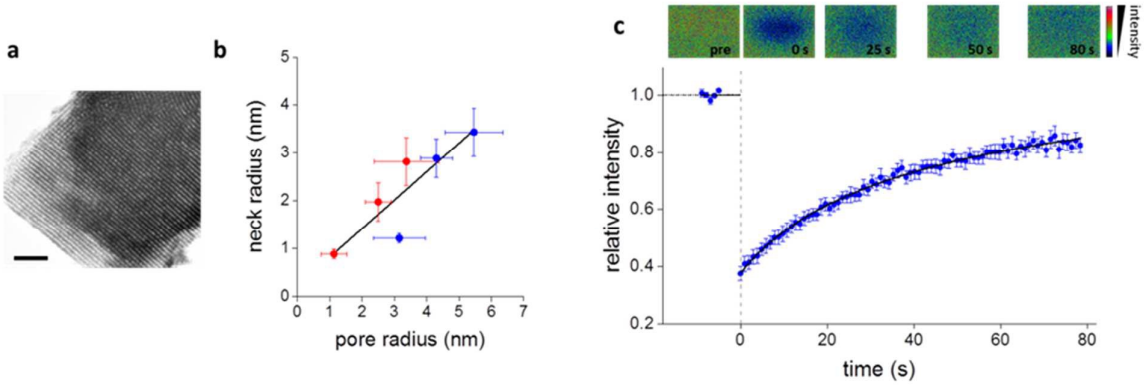

Figure 1. Characterization of TiO_2-MOTF (a) Transmission electron microscopy image of a TF400 mesoporous film. Scale bar, 100 nm (b) Pore and neck radii explored of TB (•) and TF(•) mesoporous films, solid line is only for visual guide (c) Representative fluorescence images in pseudo-color of a 16.5 x 12 μ m^2 rectangular region of a TF400 film embedded with Rhodamine B before and during the recovery of the photobleaching process (top). The recovery curve was calculated as described in the text and fitted with a biexponential function (continuous line) to obtain the dye mobile fraction.

The diffusion of molecules in highly porous frameworks can be studied using bulk approaches such as pulsed field NMR gradient[16], zero length chromatography[17], electrochemical techniques[18, 19] and localized surface plasmon resonance detection[20]. However, these ensemble methods only provide the mean behavior of molecules in these complex matrices and miss the information related to the material microheterogeneities and mechanistic details of the molecules diffusion. On the other hand, advanced fluorescence microscopy methods including single molecule tracking (c) and fluorescence correlation spectroscopy (FCS) provide analytical tools to obtain quantitative information on the diffusion of single fluorescent tracer dyes inside porous materials[21]. These methods promise a more complete in-depth understanding of mass transport in these materials as illustrated in several works from the groups of Higgins[22-26] and Bräuchle[27-29].

Here, we used FCS to study the diffusion of the fluorescent probe Rhodamine B within the pore frameworks of hydrated thin TiO_2 mesoporous films. FCS register intensity fluctuations caused by fluorescent molecules moving through the small observation volume of a confocal or two-photon excitation microscope; the correlation analysis of these fluctuations provides quantitative information on the dynamics of the molecules[30, 31].

TiO_2 films were synthesized using the EISA approach and post-processed using thermal conditioning steps for fine tuning of the pore geometry and connectivity. Basically, we used two surfactants as pore templates, Brij®58 and Pluronic® F127; mesoporous TiO_2 films were labeled as TXY, where X stands for the surfactant employed (F for Pluronic® F127 and B for Brij®58) and Y indicates the calcination temperature (in ^{o}C). The EISA approach results in thin mesoporous films (thickness ~ 100 – 200 nm) with a unidirectionally contracted *Im*3*m* 3D cubic structure; typically, TB has a pore radius in the range of 1 – 3.5 nm whereas TF pore radius is around 3.1 – 5.5 nm (Figure 1a-b and ESI). [15, 32] In particular, these mesoporous systems are characterized by an ordered array of spherical pores interconnected via smaller necks. Moreover, the body centered cubic structure *Im3m* is oriented with the [110] plane parallel to the films surface and the [1–10] perpendicular to that surface. Small angle X-ray scattering (SAXS) confirmed the mesoporous structure while environmental ellipsometric porosimetry[33] (EEP) examined the pore size distribution (i.e. pore and neck radii) and total porosity of the film (see ESI).

The dye was included within the calcined TiO_2-MOTF under a high humidity environment (~93 % HR) that guarantees water-filled pores (see ESI). Previous ellipsometric measurements rule out the presence of a water layer on top of the TiO_2 film under these humidity conditions. [6, 34, 35] As a side benefit the procedure does not require drying up the probe-embedded film, precluding or minimizing the presence of dye aggregates within the mesoporous structure. In addition TiO_2 is an excellent material compared to fully condensed mesoporous SiO_2 where dissolution processes of the matrix in aqueous solutions impose an important experimental limitation.[36]

To qualitatively assess the mobility of the dye in the hydrated TiO_2 films, we run fluorescence recovery after photobleaching (FRAP[37]) experiments in dye-embedded TF400 films. Figure 1c shows that the mobile fraction was 89 $\pm$ 4 % indicating that most of the Rhodamine B molecules diffuse freely within the film.

Then, we performed single-point FCS experiments to explore quantitatively the mobility of the probe within diffraction-limited regions of these TiO_2 films as schematized in Figure 2a; Figure 2b shows representative fluorescence autocorrelation data obtained from TF400 films.

View Article Online
DOI: 10.1039/C7CP05186G

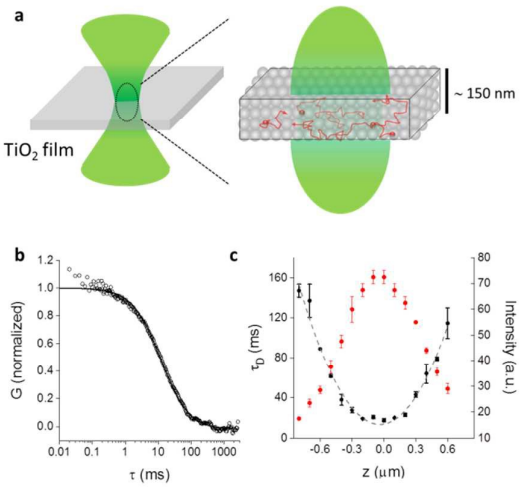

Figure 2 FCS measurements in TiO_2 films. (a) The scheme represents the laser focused on a TiO_2 film; the diffusion of dye molecules (red) in and out of the confocal volume (green oval) introduces fluctuations in the intensity trace. (b) Representative fluorescence autocorrelation curve obtained from a TF400 film. The data was fitted with Eq. 1 (continuous line) to obtain τ_D (c) Dependence of the residence time (●) and the mean intensity (●) on the focal plane (*z*), *z*= 0 was arbitrarily set as the position where the maximum intensity was registered. The dotted line shows the fitting of a parabolic function to the τ_D vs. *z* data.

The typical thickness of the mesoporous TiO_2 film is ~5 times smaller than the axial dimension of the confocal observation volume (~ 1 μm[38]) and thus, it is not possible to detect the axial motion of the Rhodamine B molecules. In line with previous works in thin samples[39], the autocorrelation data was fitted with the following equation that considers the 2D diffusion of fluorescent molecules[40]:

$$G(\tau) = \frac{1}{\langle N \rangle}\left(1+\frac{\tau}{\tau_D}\right)^{-1} \quad (1)$$

where τ_D is the characteristic diffusion time and <N> is the mean number of fluorescent particles in the observation volume.

Previous works in extremely thin samples, such as supported lipid bilayers, have shown that the laser focus should be very close to the bilayer plane for accurate FCS determinations; in other words, τ_D increases parabolically with *z* (i.e. in the optical axis direction) when moving far from the bilayer position[41]. Therefore, we run *z*-scan FCS experiments[41] and analyze the dependence of τ_D and the mean intensity with the z-position of the observation volume. Figure 2c shows that the characteristic diffusion time is approximately constant within ± 0.2-0.3 μm from the film plane and follows a parabolic-like behaviour with *z*. We did not analyze the data with the quantitative model proposed to interpret diffusion within lipid bilayers[41] due to the non-negligible thickness of the film (100-200 nm) in comparison to those bilayers (~ 5 nm) and the axial width of the point spread function. Figure 2c also shows that those *z*-positions where lowest τ_D values were registered also presented highest intensity values. Thus, the film plane could be rapidly and precisely determined by finding the *z*-position corresponding to the maximal intensity and the probe dynamics accurately recovered by single-point FCS determination at this position.

We then analyzed how the pore and neck radii modulate the mobility of the fluorescent probe within TiO_2 films subjected to different thermal conditioning and hydrated as described before. Figure 3a-b shows that the characteristic diffusion time of Rhodamine B in these films at a relatively high ionic strength (500 mM NaCl) is in the range 20-150 ms. These values were used to estimate the diffusion coefficient of the probe, *D* [42] (see Supporting Information), obtaining values that ranged from 0.2 to $1 \cdot 10^{-8}$ cm^2/s, which are in the order of those obtained in SMT experiments for non-calcined SiO_2 mesoporous thin films.[26, 27] Besides, these values are also ~ 2-3 orders lower than the unrestricted diffusion coefficient of the dye in aqueous solution (~400 10^{-8} cm^2/s). [43] Careful analysis of Figure 3a-b shows that τ_D of Rhodamine B decreases when both pore and neck radii increase. Moreover, τ_D reaches an approximately constant value of ~25 ms when pore radii are bigger than 2.8 nm (Figure 3b). The pore radii in these films (e.g. TB400, TF350 and TF400) lie in the 3-6 nm range suggesting that the diffusion of the probe within these films seems to be minimally modulated by the pore size dimensions. In addition, the faster dynamics of the probe in films with similar pore sizes but wider necks (TF200 vs. TB400) emphasizes the relevance of the neck in diffusion (see Figure 3a).

View Article Online
DOI: 10.1039/C7CP05186G

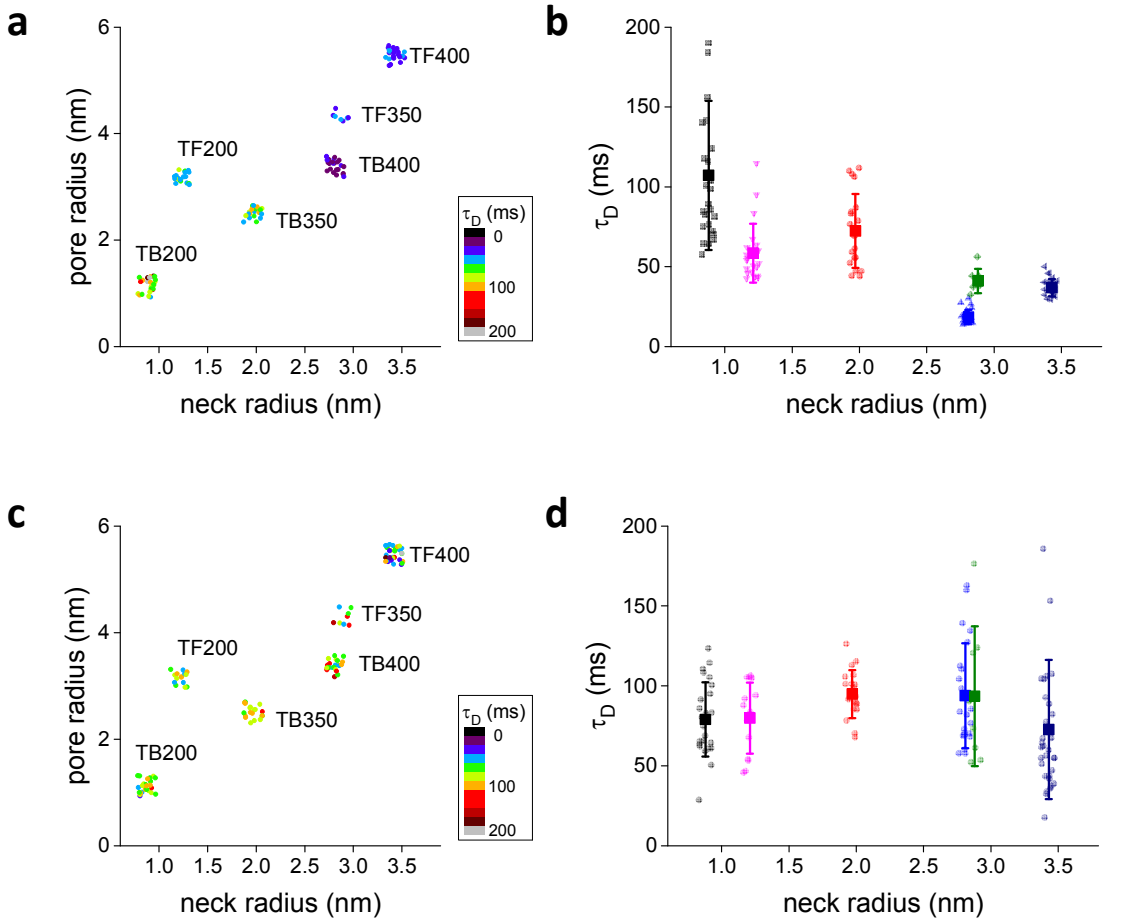

Figure 3. Rhodamine B diffusion within TiO_2-based MOTF films. The probe was incorporated in the films as described in Materials and Methods using solutions of high (a,b) or low (c,d) ionic strenght. FCS experiments were run to obtain τ_D (characteristic diffusion time) within the films pore network. The error bars in (b) and (d) represent the standard deviation of the experimental data. Colors in (b) and (d) depict the different TiO_2-MOTF studied, from left to right: TB200 (■), TF200 (■), TB350 (■) , TB400 (■), TF350 (■) and TF400 (■).

Highly confined environments with fixed surface charges impose local electrostatics constraints[44]; for instance, mesoporous TiO_2 surface charges and chemisorbed functional groups (e.g. hydrophilic and hydrophobic phosphates/phosphonates) are known to suppress the electrochemical response and diffusion of redox mediators.[45, 46] In this context, we anticipate that the ionic strength of the aqueous solutions within the TiO_2-MOTF pores will modulate the diffusion of the dye[46]. This effect is clearly seen in Figure 3c-d where τ_D does not depend on the pore and neck radii when the ionic strength of the solvent-filled pores is low. Moreover, the probe diffusion under this condition is not significantly different from that determined in mesoporous films with neck radius < 2.8 nm at high ionic strength (Figure 3b) suggesting that interactions with the pore wall slowed down the probe under these conditions. In this direction, pores with radii bigger than two Debye lengths can be safely treated in the domain of the continuum theories of electrolytes.[47]. The Debye length for 100 and 500 mM NaCl aqueous solutions are 0.96 nm and 0.21 nm respectively and, in a first approximation, we can consider that these lengths decrease the effective pore dimensions in each case. This observation implies that the effective pore neck radius at low ionic strength for all films are below the experimental 2.8 nm-threshold observed in Figure 3a; in consequence, τ_D values at low ionic strength are similar for all TiO_2 films. Interestingly, previous works showed that a significant fraction of water is structured below 2.5 nm diameter TiO_2 mesopores, while mostly free water prevails above this size[48, 49]. Thus, the effects observed above this neck diameter value are clearly attributable to electrostatics; on the other hand, we can speculate that water structuring due to confinement or minute quantities of surfactant that remains in extracted samples at 200 °C might also play a role in the probe mobility for the smaller diameter necks (see ESI, Section 2c). Recalling that the molecular size of the Rhodamine B dye (~ 1.5 nm x 1.2 nm x 0.5 nm) is comparable with the pore dimensions of TB200 and TF200 films, we presume that chemical interactions between the TiO_2 pore surface and the probe may influence the diffusion process.[25]

View Article Online
DOI: 10.1039/C7CP05186G

We then considered the estimated *D* values in each film and the corresponding pore-to-pore distance (2.2 to 11 nm from TB200 to TF400, Figure 1) to calculate the mean residence time of the probe within single pores (τ_{pore}). These values are in the 6-30 μs range and were normalized respect to the theoretical first passage time, τ_f, defined as the mean time required for the probe to travel a distance equivalent to the neck radius in aqueous solution (Figure S5). Therefore, the ratio τ_{pore} /τ_f provides the relative dwell time of the probe within the pore with respect to that expected in an unrestricted medium; likewise, the inverse of this parameter is also related to the escape probability from the pore.

Conclusions

In summary, we quantitatively described how the pore geometry and the ionic strength of the solvent-filled hydrated TiO_2 mesoporous films modulate the diffusion of a fluorescent probe. The molecular motion within the films followed normal, Fickian diffusion as expected since the spatial resolution of confocal microscopy does not allow detecting the confinement of the probe at single pores and provides information of molecules that randomly jump between adjacent pores and transverse the observation volume. Moreover, we estimated an average occupancy of ~ 10^{-3} molecules/pore in our experiments suggesting that molecules do not interfere with each other. Then, the characteristic diffusion time is an indirect measure of the escape probability from pores and is a key parameter for applications in technological areas like catalysis, sensors, environmental protection, and photovoltaics involving mesoporous films. In our experimental conditions, simple thermal conditioning steps tune the pore and neck dimensions; these parameters, in addition to the surface chemistry, are essential when analysing the dye probe interactions with the pore walls in confined environments. From this perspective, TiO_2-MOTF with precise pore dimensions and chemically tailored pore surfaces (i.e. with alkoxysilanes or phosphonic/phosphonate groups) represent promising frameworks for highly controlled diffusion/transport studies. We firmly believe that FCS and SMT constitute attractive techniques for studying *in situ* and in real time the role of interfacial chemical properties in highly porous environments. As these platforms can be directed to gating and controlled delivery, molecular recognition processes and chemical transformations, the technological consequences are far-reaching.

Conflicts of interest

There are no conflicts to declare.

Acknowledgments

This research was supported by ANPCyT (PICT 2012-0899, PICT 2012-0111, PICT 2012-2087, PICT 2015-0370, PICT 2015-0351), UBA (UBACyT 20020150100122BA), CONICET (PIP 11220130100121CO) and LNLS (Campinas, Brazil) (SAXS1-15956 project). JFA, PYS and MS acknowledge CONICET for their doctoral fellowships.

References

1. P. Innocenzi and L. Malfatti, *Chem. Soc. Rev.*, 2013, **42**, 4198-4216.
2. A. Brunsen, A. Calvo, F. J. Williams, G. J. A. A. Soler-Illia and O. Azzaroni, *Langmuir*, 2011, **27**, 4328-4333.
3. A. Walcarius, *Electroanalysis*, 2015, **27**, 1303-1340.
4. Z. Sun, G. Cui, H. Li, Y. Liu, Y. Tian and S. Yan, *J. Mater. Chem. B*, 2016, **4**, 5194-5216.
5. G. Kickelbick, *Hybrid Materials: Synthesis, Characterization, and Applications*, Wiley, 2007.
6. M. C. Fuertes, M. Marchena, M. C. Marchi, A. Wolosiuk and G. J. A. A. Soler-Illia, *Small*, 2009, **5**, 272-280.
7. A. Wolosiuk, N. G. Tognalli, E. D. Martínez, M. Granada, M. C. Fuertes, H. Troiani, S. A. Bilmes, A. Fainstein and G. J. A. A. Soler-Illia, *ACS Appl. Mater. Interfaces*, 2014, **6**, 5263-5272.
8. V. López-Puente, S. Abalde-Cela, P. C. Angelomé, R. A. Alvarez-Puebla and L. M. Liz-Marzán, *J. Phys. Chem. Lett.*, 2013, **4**, 2715-2720.
9. B. Auguié, M. C. Fuertes, P. C. Angelomé, N. L. Abdala, G. J. A. A. Soler Illia and A. Fainstein, *ACS Photonics*, 2014, **1**, 775-780.
10. I. L. Violi, M. D. Perez, M. C. Fuertes and G. J. A. A. Soler-Illia, *ACS Appl. Mater. Interfaces*, 2012, **4**, 4320-4330.
11. J. J. Nelson, T. J. Amick and C. M. Elliott, *J. Phys. Chem. C*, 2008, **112**, 18255-18263.
12. D. Song, W. Cho, J. H. Lee and Y. S. Kang, *J. Phys. Chem. Lett.*, 2014, **5**, 1249-1258.
13. A. Yella, S. Mathew, S. Aghazada, P. Comte, M. Grätzel and M. K. Nazeeruddin, *Journal of Materials Chemistry C*, 2017, **5**, 2833-2843.
14. Y. Saygili, M. Söderberg, N. Pellet, F. Giordano, Y. Cao, A. B. Muñoz-García, S. M. Zakeeruddin, N. Vlachopoulos, M. Pavone, G. Boschloo, L. Kavan, J.-E. Moser, M. Grätzel, A. Hagfeldt and M. Freitag, *Journal of the American Chemical Society*, 2016, **138**, 15087-15096.
15. G. J. A. A. Soler-Illia, P. C. Angelomé, M. C. Fuertes, D. Grosso and C. Boissiere, *Nanoscale*, 2012, **4**, 2549-2566.
16. J. Kärger, *ChemPhysChem*, 2015, **16**, 24-51.
17. A. R. Teixeira, C. C. Chang, T. Coogan, R. Kendall, W. Fan and P. J. Dauenhauer, *J. Phys. Chem. C*, 2013, **117**, 25545-25555.
18. T. C. Wei and H. W. Hillhouse, *Langmuir*, 2007, **23**, 5689-5699.
19. M. Etienne, A. Quach, D. Grosso, L. Nicole, C. Sanchez and A. Walcarius, *Chem. Mater.*, 2007, **19**, 844-856.
20. V. Gusak, L. P. Heiniger, V. P. Zhdanov, M. Grätzel, B. Kasemo and C. Langhammer, *Energy and Environmental Science*, 2013, **6**, 3627-3636.
21. S. M. Mahurin, S. Dai and M. D. Barnes, *J Phys Chem B*, 2003, **107**, 13336-13340.
22. Y. Fu, F. Ye, W. G. Sanders, M. M. Collinson and D. A. Higgins, *J Phys Chem B*, 2006, **110**, 9164-9170.
23. D. A. Higgins, S. C. Park, K.-H. Tran-Ba and T. Ito, *Annual Review of Analytical Chemistry*, 2015, **8**, 193-216.

View Article Online
DOI: 10.1039/C7CP05186G

24. E. Mei, A. M. Bardo, M. M. Collinson and D. A. Higgins, *J Phys Chem B*, 2000, **104**, 9973-9980.
25. S. C. Park, T. Ito and D. A. Higgins, *J. Phys. Chem. C*, 2015, **119**, 26101-26110.
26. F. Ye, D. A. Higgins and M. M. Collinson, *J. Phys. Chem. C*, 2007, **111**, 6772-6780.
27. F. Feil, V. Cauda, T. Bein and C. Bräuchle, *Nano Lett.*, 2012, **12**, 1354-1361.
28. B. Rühle, M. Davies, T. Bein and C. Bräuchle, *Zeitschrift fur Naturforschung - Section B Journal of Chemical Sciences*, 2013, **68**, 423-444.
29. A. Zürner, J. Kirstein, M. Döblinger, C. Bräuchle and T. Bein, *Nature*, 2007, **450**, 705-708.
30. E. L. Elson, *Methods Enzymol*, 2013, **518**, 1-10.
31. E. L. Elson, *Methods Enzymol*, 2013, **518**, 11-41.
32. P. C. Angelomé, M. Cecilia Fuertes and G. J. A. A. Soler-Illia, *Advanced Materials*, 2006, **18**, 2397-2402.
33. C. Boissiere, D. Grosso, S. Lepoutre, L. Nicole, A. B. Bruneau and C. Sanchez, *Langmuir*, 2005, **21**, 12362-12371.
34. S. Dourdain and A. Gibaud, *Applied Physics Letters*, 2005, **87**, 1-3.
35. A. Bourgeois, Y. Turcant, C. Walsh and C. Defranoux, *Applied Surface Science*, 2009, **256**, S26-S29.
36. T. Fontecave, C. Sanchez, T. Azaïs and C. Boissiére, *Chem. Mater.*, 2012, **24**, 4326-4336.
37. C. A. Day, L. J. Kraft, M. Kang and A. K. Kenworthy, *Curr Protoc Cytom*, 2012, **Chapter 2**, Unit2.19.
38. S. T. Hess and W. W. Webb, *Biophys J*, 2002, **83**, 2300-2317.
39. N. F. Y. Durand, C. Dellagiacoma, R. Goetschmann, A. Bertsch, I. Marki, T. Lasser and P. Renaud, *Anal Chem*, 2009, **81**, 5407-5412.
40. T. Kohl and P. Schwille, *Adv Biochem Eng Biotechnol*, 2005, **95**, 107-142.
41. A. Benda, M. Benes, V. Marecek, A. Lhotsky, W. Hermens and M. Hof, *Langmuir*, 2003, **19**, 4120-4126.
42. J. Ries and P. Schwille, *Bioessays*, 2012, **34**, 361-368.
43. P. O. Gendron, F. Avaltroni and K. J. Wilkinson, *Journal of Fluorescence*, 2008, **18**, 1093-1101.
44. M. Tagliazucchi and I. Szleifer, *Journal of the American Chemical Society*, 2015, **137**, 12539-12551.
45. E. H. Otal, P. C. Angelomé, S. A. Bilmes and G. J. A. A. Soler-Illia, *Advanced Materials*, 2006, **18**, 934-938.
46. D. H. Taffa, M. Kathiresan, L. Walder, B. Seelandt and M. Wark, *Phys. Chem. Chem. Phys.*, 2010, **12**, 1473-1482.
47. B. Corry, S. Kuyucak and S. H. Chung, *Chem. Phys. Lett.*, 2000, **320**, 35-41.
48. E. G. Solveyra, E. De La Llave, V. Molinero, G. J. A. A. Soler-Illia and D. A. Scherlis, *Journal of Physical Chemistry C*, 2013, **117**, 3330-3342.
49. M. I. Velasco, M. B. Franzoni, E. A. Franceschini, E. Gonzalez Solveyra, D. Scherlis, R. H. Acosta and G. J. A. A. Soler-Illia, *Journal of Physical Chemistry C*, 2017, **121**, 7533-7541.